IMPROVEMENT OF CONVECTIVE DRYING OF CARROT BY APPLYING POWER ULTRASOUND. INFLUENCE OF MASS LOAD DENSITY.

[1*]Cárcel, J.A., [1*]Garcia-Perez, J.V., [2]Riera, E., [1]Mulet, A.

[1]Grupo de Análisis y Simulación de Procesos Agroalimentarios (ASPA), Departamento de Tecnología de Alimentos. Universidad Politécnica de Valencia, Camí de Vera s/n, E46022, Valencia, Spain.

[2]Instituto de Acústica. Consejo Superior de Investigaciones Científicas, Serrano, 144, E28006, Madrid, Spain.

*Corresponding author: J. A. Cárcel, email: jcarcel@tal.upv.es

ABSTRACT

Power ultrasound is considered to be a novel and promising technology with which to improve heat and mass transfer phenomena in drying processes. The aim of this work was to contribute to the knowledge of ultrasound application to air drying by addressing the influence of mass load density on the ultrasonically assisted air drying of carrot. Drying kinetics of carrot cubes were carried out (in triplicate) with or without power ultrasound application (75 W, 21.7 kHz) at 40 ºC, 1 m/s and several mass load densities: 12, 24, 36, 42, 48, 60, 72, 84, 96, 108 and 120 kg/m^3. The experimental results showed a significant ($p<0.05$) influence of both factors, mass load density and power ultrasound application, on drying kinetics. As expected, the increase of mass load density did not affect the effective moisture diffusivity (D_e, m^2/s) but produced a reduction of the mass transfer coefficient (k, kg water/m^2/s). This was explained by considering perturbations in the air flow through the drying chamber thus creating preferential pathways and, as a consequence, increasing external mass transfer resistance. On the other hand, it was found that the power ultrasound application increased the mass transfer coefficient and the effective moisture diffusivity regardless of the mass load density used. However, the influence of power ultrasound was not significant at the highest mass load densities tested (108 and 120 kg/m^3), which may be explained from the high ratio (acoustic energy/sample mass) found under those experimental conditions. Therefore, the application of ultrasound was considered as a useful technology with which to improve the convective drying, although its effects may be reduced at high mass load densities.

Keywords: High intensity ultrasound, dehydration, modeling, effective diffusivity.

1. INTRODUCTION

Nowadays, the efficient use of energy appears to be a must. Applying power ultrasound in order to accelerate the mass transfer process is a promising technology with which to improve yields or reduce energy demand [1, 2]. Ultrasonic applications in solid-liquid systems are the most commonly employed in food processing [1,3], and among the most recent may be found the extraction of natural products [4, 5], osmotic dehydration [6] and meat [7] and cheese brining [8] or their application as pre-treatment in solid-liquid systems prior to the air drying of fruits [9-12] and vegetables [13]. Ultrasound applications in solid-gas systems are less frequent due to some practical difficulties involving energy transfer. The high impedance mismatch between the application systems and the air, which makes the acoustic wave transmission difficult, and the high attenuation of the air must be considered [14,15].

Acoustic energy assisted food drying constitutes an application of power ultrasound in solid-gas systems. The improvements associated with acoustic energy may involve several effects that lead to an increase in mass transfer during convective drying [16]. The effects may be classified according to their influence on external and/or internal resistance to mass transfer. On the one hand, boundary layer thickness may be reduced by pressure variations, oscillating velocities and microstreaming affecting the solid-gas interfaces. The aforementioned effects would involve an improvement of the water transfer rate from the solid surface to the air medium [17]. On the other hand, internal water transfer may be mainly affected by alternating expansion and compression waves produced by ultrasound in the material (a phenomenon referred to as the “sponge effect”). Ultrasound energy causes cavitation which may also affect the strongest attached moisture in the solid matrix [18]. Despite the promising effects produced by applying ultrasound in drying processes, the technical drawback of the application has made the full development of ultrasonic drying very difficult, as demonstrated by the fact that there is very little published in this issue.

Early references using sonication to improve the dehydration process date from the middle of the XX Century, promoted by the interest in the drying of heat sensitive materials [19], due to the limited heating effect of ultrasound on gas systems. Borisov and Ginkina [20] reported a series of experiments carried out in the Academy of Science of the USSR to determine the influence of the main process variables using fluid driven transducers. Da Mota and Palau [21] used a siren system to improve onion drying. A low frequency (1.6 and 3.2 kHz) was used in these experiments to partially avoid the acoustic energy attenuation; this action however, may involve an intense noise that could be an obstacle to its use.

Subsequent attempts have been made to develop new strategies for reducing not only attenuation but also impedance mismatch during drying. In this sense, Gallego-Juarez et al. [14] developed a stepped plate ultrasonic transducer to apply power ultrasound during drying. Prototypes were developed for the 10-40 kHz frequency range and power capacities of between 100 W and 1 kW for the application of airborne ultrasonic energy in different processes. For both forced-air dehydration assisted by airborne ultrasound and by direct coupling of the ultrasonic vibration to the vegetable, circular and rectangular plate transducers with a power capacity of about 100 W were used to dehydrate carrots, potatoes and mushrooms [17, 22]. When there was direct contact between the vibrating elements and the materials being dried a very intense effect was observed, which even increased when applying a low static pressure. The effect of power ultrasound on drying was reduced when the application was carried out using an air borne technique. The application to traditional convective drying technologies constitutes the main drawback of direct contact systems. Therefore, more in-depth research is needed to develop efficient ultrasonic devices that can be applied in drying.

A new air borne ultrasonic device was developed and described in previous works [23]. The design was based on the idea of using the drying chamber as the element to irradiate acoustic energy to the material being dried. In this way, no additional elements are needed to apply ultrasound during drying. The system has been found to be very effective at improving the drying rate of different products. Nevertheless, the ultrasonic effects depended on the magnitude of the process variables, such as air velocity [24, 25] and temperature [26], applied acoustic energy [27] and product properties [25]. As a consequence, the study of the influence of the process variables on the acoustic application during drying may be considered a relevant subject for research.

The main aim of this work was to address the influence of the mass load density on the acoustic drying of carrot.

2. MATERIALS AND METHODS

2.1. Ultrasonic assisted convective drier

Drying experiments were carried out using an ultrasonic assisted convective drier (Fig. 1). It involves a pilot scale convective drier [28] modified to apply ultrasound. The main modification was found in the drying chamber, since the original one (made of methacrylate) was replaced by an air borne ultrasonic device. It includes an aluminum vibrating cylinder (internal diameter 100 mm, height 310 mm and thickness 10 mm) (number 10, Fig. 1) driven by a piezoelectric composite transducer (21.8 kHz) (number 9, Fig. 1). This device was able to generate a high-intensity ultrasonic field in the air medium, reaching an average sound pressure level of 154.3 dB in stagnant air conditions. An impedance matching unit (number 13, Fig. 1) was included to electrically optimize the electric signal generated at high frequency (number 15, Fig. 1). The most important electrical parameters of the acoustic signal (voltage, intensity, frequency, power and phase) were measured using a digital power meter (WT210, Yokogawa, Japan) (number 14, Fig. 1) and logged using an application developed on LabVIEW™ (National Instruments).

Samples were placed in the drying chamber using a device made up of 10 trays (84 mm in diameter) 34 mm apart and made of a square wire mesh (side 3 mm) (number 11, Fig. 1). The dimensions were chosen in order to avoid any perturbation in the acoustic field. The device is hooked by its central axis to a sample loading chamber (number 6, Fig. 1) made of methacrylate (diameter 100 mm and height 100 mm). A sponge was used as coupling material (number 7, Fig. 1) and placed between the vibrating cylinder and the sample loading chamber in order to achieve an optimal vibration mode and avoid air losses.

The drier operated automatically; the air velocity and temperature were controlled using a PID algorithm. A balance (number 12, Fig. 1) wired to the sample loading chamber allowed the samples to be weighed at preset times by using two pneumatic moving arms (number 8, Fig. 1). The drying air was deviated from the drying chamber during weighing by using a 3-way valve (number 4, Fig. 1) to avoid any perturbation in the balance. A PC (number 16, Fig. 1) supervised the whole process.

2.2. Drying experiments

Since carrot drying has been the matter of many published articles, it was chosen as the raw material [29-31], and as such, it may be a reference material to evaluate the ultrasonic influence on mass transfer processes. Carrots (*Daucus carota* var. Nantesa) were purchased in a local market (Spanish origin). Cubic samples were obtained using a household tool. Carrot cubes were sealed in plastic films to avoid moisture loss, and maintained at 4±1 ºC until processing (storage time of under 24 hours).

The drying experiments of carrot cubes (side 8.5 mm) were carried out at 1 m/s and 40 ºC (AIR experiments). A moderate magnitude of both variables was chosen according to previous results [24-26]. The use of high air velocities could disrupt the ultrasonic field preventing the ultrasonic waves from reaching the samples [34,25]. High temperatures also reduce the relative effect of ultrasound on drying rate [26] and could affect product quality. Thus, the mild drying conditions chosen will lead not only to an increase in the drying kinetic produced by ultrasound application, but also to the preservation of product quality and energy saving. Experiments were carried out at several mass load densities; this variable was defined as the initial sample mass per unit of volume of the drying chamber. Thus, 11 levels of mass load density were tested: 12, 24, 36, 42, 48, 60, 72, 84, 96, 108 and 120 kg/m^3. In order to test the influence of power ultrasound, a batch of experiments was carried out without ultrasound application (AIR experiments) and another one with ultrasound (US experiments) by applying an electric power of 75 W to the ultrasonic transducer during air drying (Fig. 1, number 9). AIR and US experiments were replicated at least three times.

AIR and US experiments were also performed using carrot cubes (side 17 mm) to validate the modeling subsequently described in Section 2.3. In these tests, the following experimental conditions were maintained: mass load density of 36 kg/m^3 at 40 ºC and 1 m/s.

Before starting the experiments, the sealed samples were warmed for 15 min at the drying temperature. Then, the samples were unwrapped, placed on the trays and inserted in the drying chamber. Sample weight was measured at preset times (5 min).

The initial moisture content of carrots was determined according to AOAC method nº 934.06 [32] at 70 ºC and 200 mbar until constant weight.

2.3. Modeling

Water transfer during drying was described by considering the diffusion theory. The governing equation (Eq. 1) was obtained not only by considering the temperature to be uniform, but also the effective moisture diffusivity and sample volume during drying to be constant [33].

$$\frac{\partial W_p(x,y,z,t)}{\partial t} = D_e \left(\frac{\partial^2 W_p(x,y,z,t)}{\partial x^2} + \frac{\partial^2 W_p(x,y,z,t)}{\partial y^2} + \frac{\partial^2 W_p(x,y,z,t)}{\partial z^2} \right) \quad \text{(Eq. 1)}$$

where W_p is the local moisture content (kg w/kg dry matter), D_e is the average effective moisture diffusivity (m^2/s), t time (s) and x, y, z represent characteristic coordinates of cubic geometry.

In order to solve Eq. 1, uniform initial moisture content was assumed as the initial condition. Three boundary conditions were derived from the solid symmetry. By considering previous articles addressing the influence of air velocity on ultrasonic assisted air forced drying [24, 25], it was concluded that, at low air velocities like the one considered in this work (1 m/s), the external resistance to mass transfer needs to be considered to solve Eq. 1. As a consequence, three additional boundary conditions arise (Eqs. 2 to 4) from the external resistance to mass transfer in cubic geometry:

$$t > 0 \qquad x = L \qquad -D_e \rho_{ds} \frac{\partial W_p(L,y,z,t)}{\partial x} = k\left(a_w(L,y,z,t) - \varphi_{air}\right) \quad \text{(Eq. 2)}$$

$$t > 0 \qquad y = L \qquad -D_e \rho_{ds} \frac{\partial W_p(x,L,z,t)}{\partial y} = k\left(a_w(x,L,z,t) - \varphi_{air}\right) \quad \text{(Eq. 3)}$$

$$t > 0 \qquad z = L \qquad -D_e \rho_{ds} \frac{\partial W_p(x,y,L,t)}{\partial z} = k\left(a_w(x,y,L,t) - \varphi_{air}\right) \quad \text{(Eq. 4)}$$

where L represents the half length of the cubic side (m), ρ_{ds} is the dry solid density (kg dry matter/m^3), k the mass transfer coefficient (kg w/m^2/s), a_w the water activity in the solid surface and φ_{air} the relative humidity of drying air. Sorption data obtained from the bibliography were used to estimate the relationship between water activity and average moisture content for carrots [34].

Heat and mass balance in the drying air were considered in order to estimate the change in the psychometric properties of air through the bed and evaluate the degree of saturation [35]. The increase of air moisture through the bed will depend on the water evaporation rate, which is a function of drying time as well as mass load density. Thus, the maximum water evaporation rate for the early drying stages was found at the highest mass load density tested (average 0.02×10^{-3} kg/s). At this value, an increase of the air's relative humidity from 19.7 to 34% was obtained, which does not constitute a significant enough increase to slow down drying kinetics. As a consequence and in order to simplify modeling, a multilayer configuration was neglected and drying was assumed to take place in monolayer. More complex models, which take psychometric evolution through the bed into account, would be necessary in driers with higher load capacities or in ones with lower air flow rates, where higher evaporation rates could lead to air saturation.

An implicit finite difference method was used to solve Eq. 1 [36]. The set of implicit equations for the whole sub volume net was solved by programming a series of functions in Matlab® 7.1 SP3 (The MathWorks, Inc., Natick, MA, USA). The program provided both the local moisture distribution inside the solid and the average moisture content (W) of the solid, both as functions of drying time, characteristic dimension (L), effective moisture diffusivity and mass transfer coefficient.

The effective moisture diffusivity and mass transfer coefficient were simultaneously identified from the experimental data using the SIMPLEX method [35]. The objective function to be minimized was the sum of the squared differences between the experimental and the calculated average moisture content.

In order to evaluate the fit of the models, the explained variance (VAR, Eq. 5) and the mean relative error were computed (MRE, Eq. 6). The joint interval confidences (95 % statistical significance) were also calculated in order to estimate the consistency of the simultaneous identification of both parameters [37].

$$VAR = \left[1 - \frac{S_{tW}^2}{S_W^2}\right] \cdot 100 \qquad \text{(Eq. 5)}$$

$$\mathrm{MRE} = \frac{100}{N}\left[\sum_{i=1}^{N} \frac{\left|W_{ei} - W_{ci}\right|}{W_{ei}}\right] \qquad \text{(Eq. 6)}$$

where S^2_W and S^2_{tW} are the variance of the sample and the estimation, respectively, W_{ei} and W_{ci} are the experimental and calculated average moisture contents and N the number of experimental data.

The analysis of variance (ANOVA) was carried out and LSD intervals ($p<0.05$) were estimated using Statgraphics® Plus 5.1 (StatPoint, Inc., Warrenton, VI, USA) to evaluate the significant influence of sonication on D_e and k parameters.

3. RESULTS AND DISCUSSION

3.1. Experimental drying kinetics

AIR and US drying kinetics of carrot cubes obtained at several mass load densities are plotted in Fig. 2 and Fig. 3, respectively. Experimental results showed an influence of mass load density on drying rate. The effect was similar regardless of whether AIR or US experiments were considered; the lower the mass load density, the higher the drying rate. In AIR experiments, when mass load density was increased from 12 to 120 kg/m^3, the drying time needed to reach a moisture content of 1 (kg w/kg dm) went up by 50 %. An identical rise was found for sonicated samples (US experiments). A similar influence of mass load density was found on the microwave drying of carrot slices [38].

Once the influence of mass load density on air drying saturation through the bed (see Section 2.3) is neglected, the influence on the drying rate may be explained by considering its effect on the external resistance to mass transfer. The increase in the amount of samples on the trays may introduce fluctuations in the air flow creating preferential pathways and, therefore, increasing this resistance. Indeed, this effect would increase as the mass load density got higher.

The application of power ultrasound affected the drying kinetics (Fig. 4). Sonicated samples presented lower moisture contents at the same experimental time. Therefore, the drying rate increased when ultrasound was applied. It seems that the influence of power ultrasound was similar at high and low mass load densities (Fig. 4), representing a reduction of approximately 30 % in the total drying time. The improvement in drying kinetics when power ultrasound is applied during drying has already been reported for carrots [15-16,25-27], as well as for other products, such as potatoes and mushrooms [17,22], persimmon [24,25] and lemon peel [25,27]. To improve convective drying, it may be also highlighted the application of power ultrasound in liquid media [13]. This technology may be considered a product's pre-treatment prior to the drying process, the structural changes induced in the material by the ultrasonic application [39] facilitate the subsequent convective drying process. The drying kinetics of melons [9], sapota [10], banana [11], pineapple [12], mushrooms, Brussels sprouts, and cauliflower [13] have been accelerated by the application of power ultrasound as a pre-treatment prior to the drying process. The ultrasonic pre-treatment involved an average reduction (10 %) of the total drying time for banana [11] and pineapple [12]. This reduction was lower than both that the reported in this work when using ultrasonic assisted drying for carrots (30 %) or also that previously reported in the literature for a fruit like persimmon (40 %) [25]. Ultrasonic assisted drying does not only affects the product's microstructure, but also the mass transfer processes that take place during drying. Therefore, the effects are more intense than when ultrasound is applied as a pre-treatment, where the effect on the drying kinetic is linked to the microstructural changes induced by ultrasound. Finally, it should be pointed out that in order to optimize the drying process thus reducing drying time, both ultrasonic alternatives may be combined. Thereby, an ultrasonic pre-treatment followed by ultrasonic assisted drying could bring about a drastic reduction in drying time.

From the experimental results, the influence of power ultrasound on the mass transfer process which takes place during the convective drying of carrot cubes cannot be fully addressed, since ultrasonic influence may affect external or/and internal resistance. In addition, the ultrasonic influence needs to be quantified. Modeling may be considered not only a useful tool with which to clarify these issues, but also one that may be used to predict the behaviour of the system under different operational conditions [40], which is very useful in drier design and optimization.

3.2. Modeling

3.2.1. Results

The drying kinetics of carrot cubes were modeled following the diffusion theory. External resistance to mass transfer was considered in the model, as previously noted. Average effective moisture diffusivities (D_e) and mass transfer coefficients (k) identified from the non-linear optimization method considered are presented in Table 1 according to the mass load in question.

The D_e values obtained were close to others found in literature for the convective drying of this product [26,29-31]. A wide dispersion was found for the D_e figures within the same kind of experiment, AIR or US (Fig. 5), which may be explained by considering the particular structure of carrots. Srikiatden and Roberts [29] reported significant differences for the D_e figures in the hot air drying of carrot core and cortex. Therefore, carrot is considered to be a heterogeneous material not only due to its variable vegetal matrix but also to its structure, which explains the variability observed in the experimental results. There was no observed pattern of the values linked to mass load.

In the case of the mass transfer coefficient (k), the values found are in the same order of magnitude as those identified when modeling the drying of other foodstuffs assuming external resistance and similar air flow rates [36,41,42].

A multifactor ANOVA was carried out to evaluate whether the D_e values identified for AIR and US experiments were significantly different ($p<0.05$). The factors considered in the analysis were the mass load density (11 levels: 12, 24, 36, 42, 48, 60, 72, 84, 96, 108 and 120 kg/m^3) and the application of power ultrasound (2 levels: with or without ultrasound application). A similar ANOVA was carried out for the mass transfer coefficient (k). The LSD (least significance difference) intervals were estimated in order to identify significantly different ($p<0.05$) groups.

3.2.2. *Influence of mass load density*

Mass load density did not significantly ($p<0.05$) influence effective moisture diffusivity in either AIR experiments or US experiments (Table 1). Indeed, internal resistance cannot be affected by this variable since internal water movement does not depend on particles loaded in the drying chamber.

The influence of mass load on the convective drying rate may be considered in the external resistance to mass transfer, as was previously noticed from experimental data. The identified mass transfer coefficients confirmed this assumption since they showed there was a significant ($p<0.05$) influence of mass load density (Table 1; Fig. 6). This parameter was observed to behave in a similar way in both AIR and US experiments: the higher the k figures, the lower the mass load densities (Fig. 6). Nevertheless, there is a seeming tendency of the values to remain constant for mass load densities higher than 90 kg/m^3. Higher mass load densities could not be tested since 120 kg/m^3 corresponds to the maximum amount of particles on the trays for a monolayer distribution.

3.2.3. ***Influence of power ultrasound application.***

Power ultrasound application had a significant ($p<0.05$) influence on effective moisture diffusivity (Table 1; Fig. 5). Sonicated samples (US experiments) presented an average D_e figure of 2.88x10^{-10} m^2/s, which was significantly ($p<0.05$) higher than that found in AIR experiments (2.06x10^{-10} m^2/s) (Fig. 5). Sonication led to a 40 % improvement in this parameter, regardless of the mass load at the amounts tested. Therefore, ultrasound application reduced the internal resistance to mass transfer in the convective drying of carrots, thus improving internal water movement. Alternating expansion and contraction cycles produced by ultrasonic waves in the material (sponge effect) [14] may contribute to water leaving the solid matrix. The cavitation phenomenon may even help to remove the strongest attached moisture.

Previous results reported that the influence of power ultrasound on the internal resistance to mass transfer is heavily dependent on the internal structure of the material [25,27]. Porosity is one of the variables which most heavily influences the effects of the acoustic energy on drying processes. High porosity products present a low internal resistance due to large intercellular spaces; as a consequence, the acoustic energy levels needed to affect water removal during drying are lower than in low porosity products [25,27]. Carrot is considered a low porosity (0.04) material if compared with other biological products like lemon peel (porosity 0.40) [43], therefore, if the same acoustic intensity level is applied, the acoustic effects are more intense in drying kinetics of lemon peel than carrot. This fact has already been reported in the literature [25, 27].

External resistance was also affected by power ultrasound application. The mass transfer coefficients identified in US experiments were significantly higher than those found in AIR experiments at the mass load densities tested (Table 1; Fig. 6). However, LSD intervals ($p<0.05$) in both AIR and US experiments overlapped for mass load densities of over 90 kg/m^3 (Fig. 6). This fact could be linked to the reduction of the ratio (acoustic energy/sample mass) as the load density was higher, thus providing less intense acoustic effects. Another aspect to take into consideration is that mass transfer is proportional to transfer area, which is affected by loading, due to the fact that particles being in contact also perturb the transport process. Further research would be needed in order to test these hypotheses.

The influence of power ultrasound on the external resistance to mass transfer may be explained from its effect on the diffusion boundary layer. Power ultrasound introduces pressure variations, oscillating velocities and microstreaming at the gas-solid interfaces thus reducing boundary layer thickness and, therefore, improving water transfer from the solid surface to air medium [14, 17]. This effect would only be significant during drying if external resistance was involved in drying control, which is the case under the experimental conditions used in these experiments [24, 25].

3.2.4. ***Model fitting and validation***

The proposed diffusion model adequately described the drying kinetics under the different experimental conditions used in this work, thus providing relevant information about the influence of mass load density and power ultrasound application on the convective drying of carrots. Modeling provided percentages of explained variance of over 99% and mean relative errors of under 6% in every case. Both parameters confirm an adequate description of drying kinetics (Table 1). Fig. 4 shows how the model fitted the experimental data and how it provided a good description of the moisture behavior during drying under different experimental conditions. Both experimental moisture contents and those calculated using the diffusion model are depicted together for a specific experiment in Fig. 7. The similarity between the experimental and calculated data may be observed from both Fig. 4 and 7, which again shows the suitability of the diffusion model to describe the drying kinetics under these experimental conditions.

To test the robustness of the results and, therefore, the ability of the diffusion model used in this work to extrapolate the drying of carrots under other conditions, drying experiments were carried out using 17 mm long carrot cubes at 40 ºC, 1 m/s and 36 kg/m^3. Since the kinetic parameters are independent of particle size, the drying kinetics were simulated using the proposed diffusion model, considering a thickness of 17 mm, from the average k and D_e figures identified for carrot cubes of side 8.5 mm (Table 1) for AIR and US experiments and the same mass load density (36 kg/m^3). The simulated curves are compared to experimental data in Fig. 8 and it can be observed that the model allowed the drying of these samples to be accurately predicted. The simulated results are close to the experimental data in both AIR and US curves. This result shows the ability of the results found in this work to simulate the drying of carrot at 40 ºC and 1 m/s with or without ultrasonic application over a wide range of mass load densities (from 12 to 120 kg/m^3). Furthermore, the proposed model could be very useful for optimization stages.

4. CONCLUSION

The sonication involved a significant improvement of mass transfer processes during the convective drying of carrot cubes over a wide range of mass load densities (12-120 kg/m^3). As expected, effective moisture diffusivity (an internal property of the material) remained constant in line with mass load density and the average value in the US experiments was significantly higher than in the AIR experiments. An increase in the mass load density reduced the mass transfer coefficient, which was probably linked to an increase in the external resistance to mass transfer. Sonication produced a significant increase in the mass transfer coefficient. This increase is reduced at high mass load densities, in all likelihood due to the reduction of the ratio (acoustic energy/sample mass) or the transfer area available in the particles.

5. ACKNOWLEDGMENTS

The authors would like to acknowledge the financial support of the Spanish Ministry of Science and Technology (DPI2009-14549-C04-04) and the Universidad Politécnica de Valencia (PAID-06-08- 3180).

6. REFERENCES

1. Mason, T.J.; Paniwnyk, L.; Lorimer, J.P. The use of ultrasound in food technology. Ultrasonics Sonochemistry 1996, 3, S253-S256.

2. Mason, T.J.; Power ultrasound in food processing. The way forward. In Ultrasound in Food Processing; Povey, M.J.W., Mason, T.J. Eds.; Chapman & Hall: London, 1998; 105-126.

3. Mason, T.J.; Lorimer, J.P. Applied sonochemistry. The uses of power ultrasound in chemistry and processing; Wiley-VCH; Weinheim, 2002.

4. Riera, E.; Golas, Y.; Blanco, A.; Gallego-Juarez, J.A.; Blasco, M.; Mulet, A. Mass transfer enhancement in supercritical fluids extraction by means of power ultrasound. Ultrasonics Sonochemistry 2004, 11, 241-244.

5. Cravotto, G.; Boffa, L.; Mantegna, S.; Perego, P.; Avogadro, M.; Cintas, P. Improved extraction of vegetable oils under high-intensity ultrasound and/or microwaves. Ultrasonics Sonochemistry 2008, 15, 898-902.

6. Cárcel, J.A.; Benedito, J.; Rosselló, C.; Mulet, A. Influence of ultrasound intensity on mass transfer in apple immersed in a sucrose solution. Journal of Food Engineering 2007, 78, 472-479.

7. Cárcel, J.A.; Benedito, J.; Bon, J.; Mulet, A. High intensity ultrasound effects on meat brining. Meat Science 2007, 76, 611-619.

8. Sánchez, E.S.; Simal, S.; Femenia, A.; Benedito, J.; Rosselló, C. Influence of ultrasound on mass transport during cheese brining. European Food Research and Technology 1999, 209, 215-219.

9. Rodrigues, S., Fernandes, F.A.N. Use of ultrasound as pretreatment for dehydration of melons. Drying Technology 2007, 25, 1791-1796.

10. Fernandes, F.A.N., Rodrigues, S. Dehydration of sapota (Achras sapota L.) using ultrasound as pretreatment. Drying Technology 2008, 26, 1232-1237.

11. Fernandes, F.A.N, Rodrigues, S. Ultrasound as pre-treatment for drying of fruits: Dehydration of banana. Journal of Food Engineering 2007, 82, 261-267.

12. Fernandes, F.A.N, Linhares, F.E., Rodrigues, S. Ultrasound as pre-treatment for drying of pineapple. Ultrasonics Sonochemistry 2008, 15, 1049-1054.

13. Jambrak, A.R., Mason, T.J., Paniwnyk, L., Lelas, V. Accelerated drying of button mushrooms, Brussels sprouts and cauliflower by applying power ultrasound and its rehydration properties. Journal of Food Engineering 2007, 81, 88-97.

14. Gallego-Juárez, J.A., Rodríguez-Corral, G., Gálvez-Moraleda, J.C., Yang, T.S. A new high intensity ultrasonic technology for food dehydration. Drying Technology 1999, 17, 597-608.

15. Mulet., A.; Cárcel, J.A.; Sanjuán, N.; Bon, J. New food drying technologies-Use of ultrasound. Food Science and Technology International 2003, 9, 215-221.

16. Gallego-Juárez, J.A. Some applications of air-borne power ultrasound to food processing. In Ultrasound in Food Processing; Povey, M.J.W.; Mason, T.J., Eds.; Chapman & Hall; London, 1998, 127-143.

17. Gallego-Juárez, J.A.; Riera, E.; De la Fuente, S.; Rodríguez-Corral, G.; Acosta-Aparicio, V.M.; Blanco, A. Application of high-power ultrasound for dehydration of vegetables: processes and devices. Drying Technology 2007, 25, 1893-1901.

18. Muralidhara, H.S.; Ensminger, D.; Putnam, A. Acoustic dewatering and drying (low and high frequency): State of the art review. Drying Technology 1985, 3, 529-566.

19. Boucher, R.M.G. Drying by airborne ultrasonics. Ultrasonics News 1959, 3, 8.

20. Borisov, Y.Y.; Gynkina, N.M. Acoustic drying. In Physical principles of ultrasonic technology. Rozenberg, L.D. Ed.; Plenum Press: New York, 1973.

21. Da Mota, V. M.; Palau, E. Acoustic drying of onion. Drying Technology 1999, 17, 855-867.

22. De la Fuente, S.; Riera, E.; Acosta, V.M.; Blanco, A.; Gallego-Juárez, J.A. Food drying process by power ultrasound. Ultrasonics 2006, 44, e523-e527.

23. García-Pérez, J.V.; Cárcel, J.A.; De la Fuente, S.; Riera, E. Ultrasonic drying of foodstuff in a fluidized bed. Parametric study. Ultrasonics 2006, 44, e539-e543.

24. Cárcel, J. A.; García-Pérez, J. V.; Riera, E.; Mulet, A. Influence of high intensity ultrasound on drying kinetics of persimmon. Drying Technology 2007, 25, 185-193.

25. García-Pérez, J.V.; Cárcel, J.A.; Benedito, J.; Mulet, A. Power ultrasound mass transfer enhancement in food drying. Food and Bioproducts Proccessing, 2007, 85, 247-254.

26. García-Pérez, J.V.; Rosselló, C.; Cárcel, J.A.; De la Fuente, S.; Mulet, A. Effect of air temperature on convective drying assisted by high power ultrasound. Defect and Diffusion Forum 2006, 258-260, 563-574.

27. Garcia-Perez, J.V.; Carcel, J.A.; Riera, E.; Mulet, A. Influence of the applied acoustic energy on the drying of carrots and lemon peel. Drying Technology 2009, 27, 281-287.

28. Bon, J.; Simal, S.; Rosselló, C.; Mulet, A. Drying characteristics of hemispherical solids. Journal of Food Engineering 1997, 34, 109-122.

29. Srikiatden, J.; Roberts, S.S. Measuring moisture diffusivity of potato and carrots (core and cortex) during convective hot air and isothermal drying. Journal of Food Engineering 2006, 74, 143-152.

30. Ruiz-López, I.I.; Córdova, A.V.; Rodríguez-Jimenes, G.C.; García-Alvarado, M.A. Moisture and temperature evolution during food drying: effect of variable properties. Journal of Food Engineering 2004, 63, 117-124.

31. Mulet, A.; Berna, A.; Rosselló, C. Drying of carrots I. Drying models. Drying Technology 1989, 7, 537-557.

32. AOAC. Official methods of analysis. Association of Official Analytical Chemist: Arlington, 1997.

33. Simal, S.; Femenia, A.; García-Pascual, P.; Rosselló, C. Simulation of the drying curves of a meat-based product: effect of the external resistance to mass transfer. Journal of Food Engineering 2003, 58, 193-199.

34. Zhang, X.W.; Liu, X.; Gu, D.X.; Zhou, W.; Wang, R.L.; Liu, P. Desorption isotherms of some vegetables. Journal of Science of Food and Agriculture 1996, 40, 303-306.

35. Garcia-Perez, J.V.; Carcel, J.A.; García-Alvarado, M.A.; Mulet, A. Simulation of grape stalk deep bed drying. Journal of Food Engineering 2009, 90, 308-314.

36. Mulet, A.; Blasco, M.; García-Reverter, J.; García-Pérez, J.V. Drying kinetics of Curcuma longa rhizomes. Journal of Food Science 2005, 7, E318-E323.

37. Garcia-Alvarado, M.A.; De la Cruz-Medina, J.; Waliszewski-Kubiak, K.; Salgado-Cervantes, M.A. Statistical analysis of the Gab and Henderson equations for sorption isotherms of foods. Drying Technology 1996, 13, 2141-2152.

38. Wang, J.; Xi, Y.S. Drying characteristics and drying quality of carrot using a two-stage microwave process. Journal of Food Engineering 2005, 68, 505-511.

39. Fernades, F.A.N., Gallao, M.I., Rodrigues, S. Effect of osmotic dehydration and ultrasound pre-treatment on cell structure: Melon dehydration. LWT - Food Science and Technology, 2008, 41, 604-610.

40. Sanjuán, N.; Lozano, M.; García-Pascual, P.; Mulet, A. Dehydration kinetics of red pepper (*Capsicum annuum* L var Jaranda). Journal of the Science of Food and Agriculture 2003, 83, 697-701.

41. Krokida M.K.; Maroulis, Z.B.; Marinos-Kouris, D. Heat and mass transfer coefficients in drying: compilation of literature data. Drying Technology 2002, 20, 1-18.

42. Bialobrzewski, I. Determination of the mass transfer coefficient during hot-air-drying of celery root. Journal of Food Engineering 2007, 78, 1388-1396.

43. Boukouvalas, Ch.J.; Krokida, M.K.; Maroulis, Z.B.; Marinos-Kouris, D. Density and porosity: literature data compilation for foodstuffs. International Journal of Food Properties 2006, 9,: 715-746.

7. FIGURE CAPTIONS

Fig. 1. Diagram of the ultrasonic assisted drier. 1. Fan, 2. Heating unit, 3. Anemometer, 4. 3-Way valve, 5. Thermocouple, 6. Sample loading chamber, 7. Coupling material, 8. Pneumatic moving arms, 9. Ultrasonic transducer, 10. Vibrating cylinder, 11. Trays, 12. Balance. 13. Impedance matching unit, 14. Wattmeter, 15. High power ultrasonic generator, 16. PC.

Fig 2. AIR drying kinetics of carrot cubes (side 8.5 mm) at 40 ºC, 1 m/s and different mass load densities: (▲) 12; (-) 24; (∆) 36; (◊) 72; (□) 84; (■) 108; (x) 120 kg/m^3.

Fig 3. US (75 W, 21.7 kHz) drying kinetics of carrot cubes (side 8.5 mm) at 40 ºC, 1 m/s and different mass load densities: (▲) 12; (-) 24; (∆) 36; (◊) 72; (□) 84; (■) 108; (x) 120 kg/m^3.

Fig. 4. AIR and US (75 W, 21.7 kHz) drying kinetics of carrot cubes (side 8.5 mm) at 40 ºC, 1 m/s and the same mass load density: (∆ US; ▲ AIR) 12 kg/m^3; (□ US, ■ AIR) 120 kg/m^3, (___) model.

Fig. 5. Effective moisture diffusivities (D_e) identified using the diffusion model considering external resistance for AIR (∆ -----) and US (▲——) experiments.

Fig. 6. Mass transfer coefficients (k) identified using the diffusion model considering external resistance for AIR (∆) and US (▲) experiments.

Fig. 7. Experimental moisture content versus that calculated using the diffusion model. AIR experiment carried out at 40 ºC, 1 m/s and 60 kg/m^3.

Fig. 8. Simulation of AIR and US drying kinetics of carrot cubes (side 17 mm) and comparison with experimental data. Simulation (___), AIR (□) and US (o).

8. TABLES

Table 1. Modeling drying kinetics of carrot cubes. Parameters estimated and statistical results obtained.

Mass load density (kg/m^3)	**AIR** D_e (10^{-10} m^2/s)	**AIR** k (10^{-4} kg w/m^2/s)	**AIR** VAR (%)	**AIR** MRE (%)	**US** D_e (10^{-10} m^2/s)	**US** k (10^{-4} kg w/m^2/s)	**US** VAR (%)	**US** MRE (%)
12	$1.84\pm0.28_{a}$	$5.28\pm0.46_{uv}$	99.4	5.5	$2.51\pm0.50_{ab}$	$6.24\pm0.99_{t}$	99.6	4.0
24	$2.11\pm0.80_{a}$	$4.37\pm1.07_{uvw}$	99.9	2.7	$2.76\pm0.37_{ab}$	$5.33\pm0.54_{tuz}$	99.6	2.7
36	$2.20\pm0.28_{ab}$	$3.80\pm0.80_{vwxz}$	99.9	1.5	$3.06\pm0.27_{b}$	$4.94\pm0.83_{uvz}$	99.9	1.6
42	$2.32\pm0.50_{ab}$	$3.51\pm0.20_{vwxyz}$	99.9	1.4	$2.82\pm0.66_{ab}$	$4.82\pm0.69_{uvz}$	99.9	1.2
48	$1.97\pm0.24_{a}$	$3.58\pm0.71_{vwxyz}$	99.9	1.7	$2.54\pm0.08_{ab}$	$4.71\pm0.91_{uvz}$	99.9	1.9
60	$1.87\pm0.38_{a}$	$2.92\pm0.51_{wxy}$	99.9	1.4	$2.53\pm0.26_{ab}$	$4.39\pm0.28_{uvwz}$	99.9	1.4
72	$1.78\pm0.22_{a}$	$2.90\pm0.46_{wxy}$	99.9	1.9	$2.69\pm0.03_{ab}$	$3.93\pm0.22_{uvwz}$	99.9	1.1
84	$1.66\pm0.34_{a}$	$2.59\pm0.20_{wxy}$	99.8	2.5	$3.20\pm0.21_{b}$	$3.42\pm0.55_{vwxyz}$	99.9	1.6
96	$2.37\pm0.17_{ab}$	$2.81\pm0.36_{wxy}$	99.9	1.0	$3.46\pm0.37_{b}$	$3.11\pm0.60_{wxy}$	99.8	1.9
108	$2.31\pm0.65_{ab}$	$2.38\pm0.18_{wxy}$	99.9	1.5	$3.27\pm0.37_{b}$	$2.77\pm0.21_{wxy}$	99.8	2.3

Subscripts (a, b) and (t, u, v, w, x, y, z) show homogeneous groups established from LSD intervals ($p<0.05$).

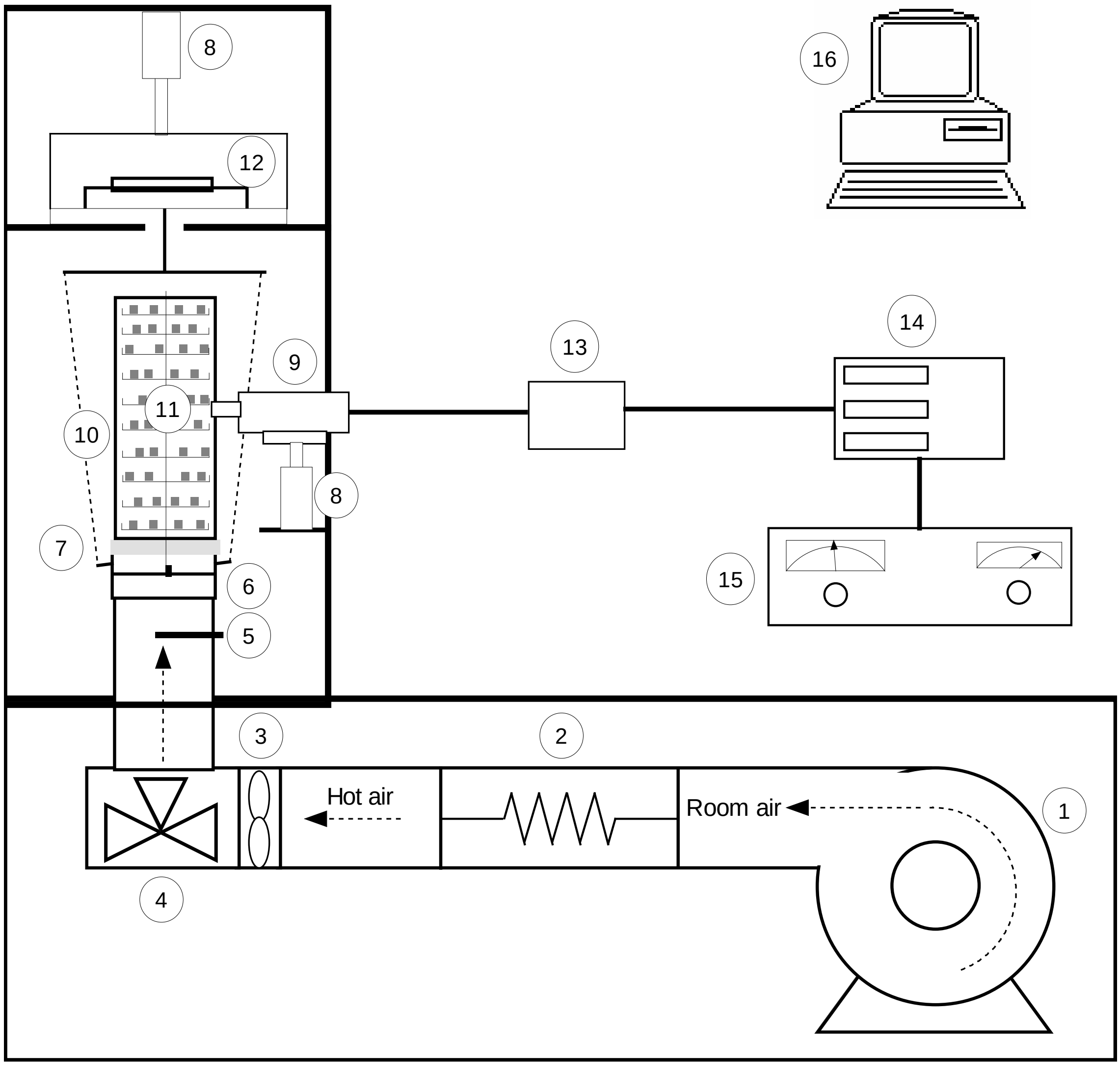

Fig. 1.

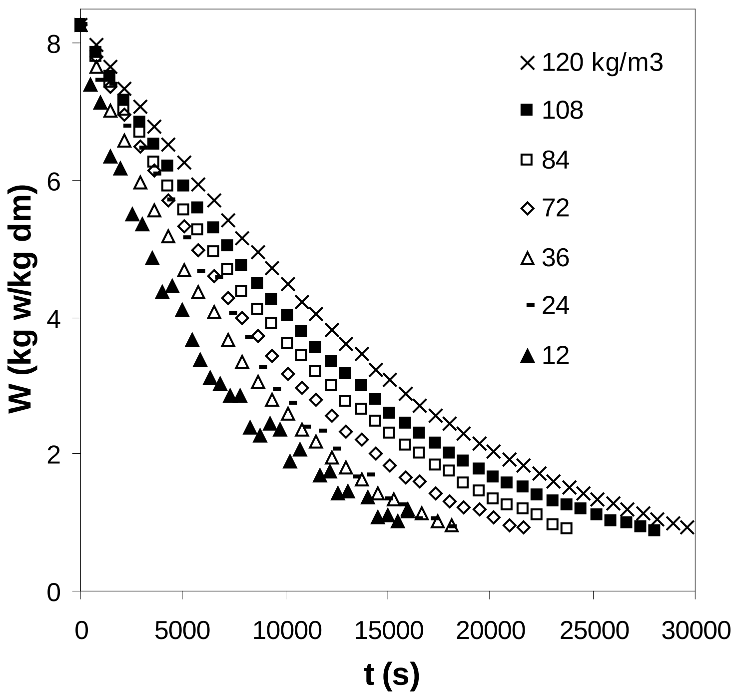
W (kg w/kg dm)
t (s)
0
2
4
6
8
0
5000
10000
15000
20000
25000
30000
120 kg/m3
108
84
72
36
24
12

Fig. 2

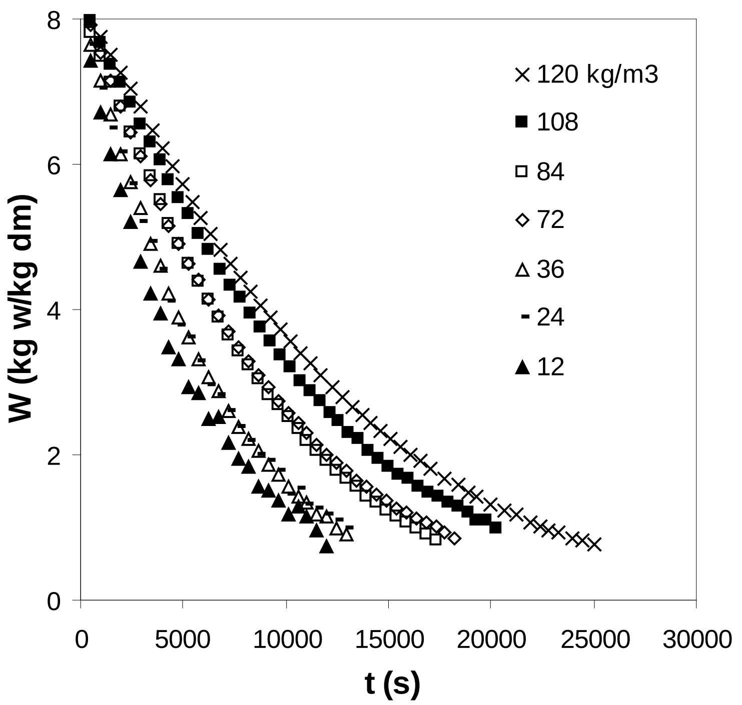
W (kg w/kg dm)
0
2
4
6
8
t (s)
0
5000
10000
15000
20000
25000
30000
120 kg/m3
108
84
72
36
24
12

Fig. 3

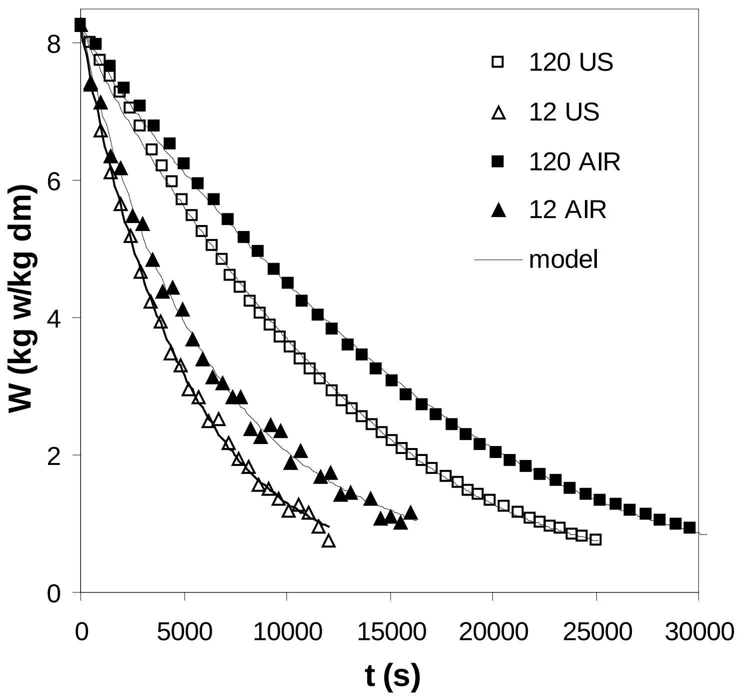
W (kg w/kg dm)
t (s)
0
2
4
6
8
0
5000
10000
15000
20000
25000
30000
120 US
12 US
120 AIR
12 AIR
model

Fig. 4

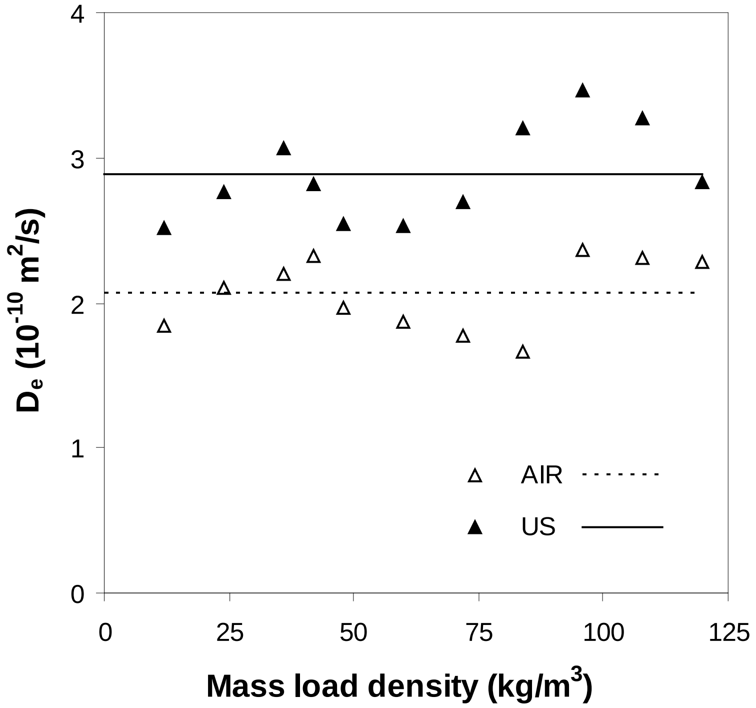

De (10-10 m2/s)
Mass load density (kg/m3)
0
1
2
3
4
0
25
50
75
100
125
AIR
US

Fig. 5

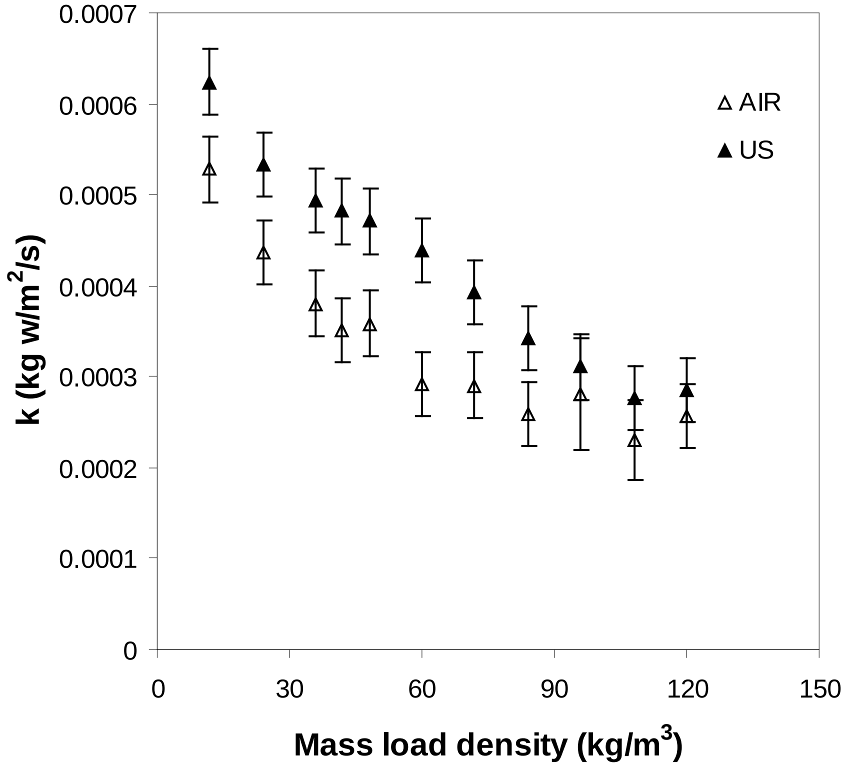

0.0007
0.0006
0.0005
0.0004
0.0003
0.0002
0.0001
0
k (kg w/m2/s)
0
30
60
90
120
150
Mass load density (kg/m3)
AIR
US

Fig. 6

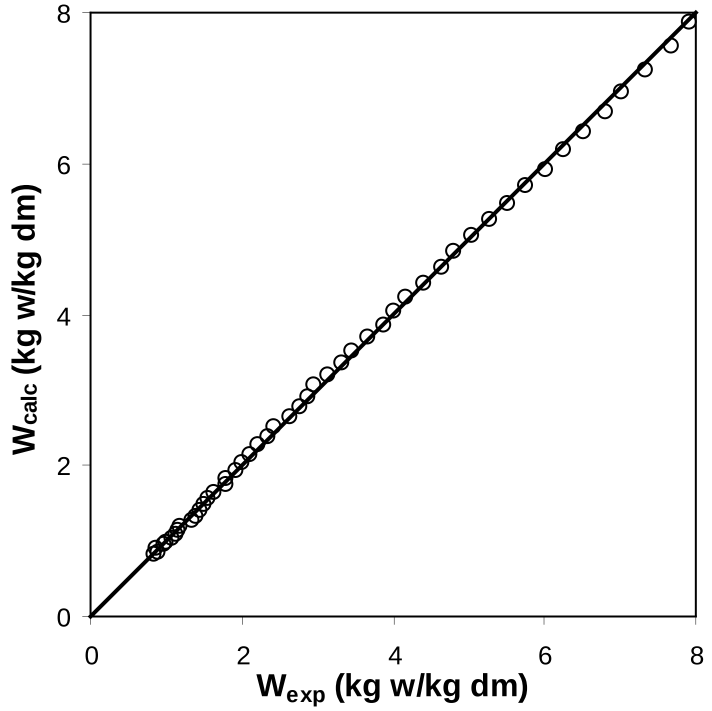

Fig. 7

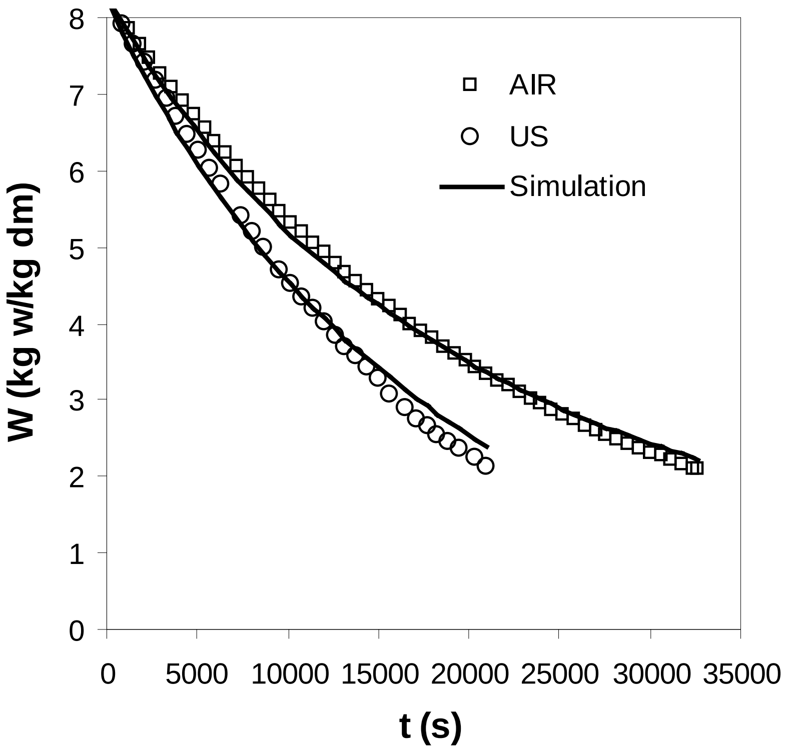
AIR
US
Simulation
W (kg w/kg dm)
t (s)
0
1
2
3
4
5
6
7
8
0
5000
10000
15000
20000
25000
30000
35000

Fig. 8